

# Cosmological dynamics of dark energy in scalar-torsion $f(T, \phi)$ gravity

Manuel Gonzalez-Espinoza,<sup>a</sup> and Giovanni Otalora<sup>a</sup>

<sup>a</sup>Instituto de Física, Pontificia Universidad Católica de Valparaíso,  
Casilla 4950, Valparaíso, Chile

E-mail: [manuel.gonzalez@pucv.cl](mailto:manuel.gonzalez@pucv.cl), [giovanni.otalora@pucv.cl](mailto:giovanni.otalora@pucv.cl)

**Abstract.** It is investigated the cosmological dynamics of scalar-torsion  $f(T, \phi)$  gravity as a dark energy model. We concerned about the phenomenology of model  $f(T, \phi) = -T/2\kappa^2 - F(\phi)G(T) - V(\phi)$ , with  $F(\phi) \sim e^{-\sigma\kappa\phi}$ ,  $V(\phi) \sim e^{-\lambda\kappa\phi}$  and  $G(T) \sim T^{1+s}$ . We obtain the critical points of the autonomous system, along with the stability conditions of each one of them and their cosmological properties. Particularly, we show the existence of new scaling solutions in which the energy density of dark energy scales as the background fluid density, thus, defining the so-called scaling radiation and scaling matter epochs. As well, we have found new critical points which are attractors with accelerated expansion but these scaling solutions are unstable fixed points and, therefore, the system exits these solutions toward attractors points describing the dark energy dominated era at the current epoch of cosmic acceleration.

---

## Contents

<b>1</b>	<b>Introduction</b>	<b>1</b>
<b>2</b>	<b>Teleparallel Gravity</b>	<b>2</b>
<b>3</b>	<b>Scalar-Torsion <math>f(T, \phi)</math> Gravity</b>	<b>4</b>
<b>4</b>	<b>Dynamical system</b>	<b>6</b>
<b>5</b>	<b>Critical Points</b>	<b>8</b>
<b>6</b>	<b>Stability of critical points</b>	<b>10</b>
<b>7</b>	<b>Numerical results</b>	<b>13</b>
<b>8</b>	<b>Concluding Remarks</b>	<b>18</b>

---

## 1 Introduction

The discovery that the Universe is expanding at an accelerated rate, through the analysis of observational data of supernovas Ia [1, 2], radically modified our understanding of Cosmology because it indicated the existence of a new component that occupies the 68 % of our Universe. Even more, this new component remains a mystery due the fact that its true nature is still unknown and that is why it adopts the name of dark energy. Nonetheless, the Standard Cosmology presents us an excellent model when we consider the vacuum energy, represented as a cosmological constant at the Einstein equations, as the responsible for the accelerated expansion of our Universe. This  $\Lambda$ CDM model (cosmological constant  $\Lambda$  and cold dark matter) is an excellent model to describe Dark Energy and it provides us with a good description of the observational data for the astronomy, astrophysics and cosmology. But, the latest observational data has pointed out some tensions or anomalies which are of statistical importance [3–6]. Particularly, the tension between the Planck experiment and other low-redshift probes at the measurement of the anisotropy of the Cosmic Microwave Background (CMB), the tension of the Hubble at the present time  $H_0$  [3–6], the tension at the measurement of the amplitude  $\sigma_8$  and the growth rate of cosmic structure  $f\sigma_8$  [3–6], etc. And although, this could imply systematic errors in the method to obtain data, this also could indicate the necessity of a new cosmological model. There is a lot of research work in the investigation of this tension [7–10] but models with a modified matter source described by a scalar field -such as quintessence [11], k-essence [12], Galileons [13, 14], etc- are proving to be good alternatives for dark energy. Particularly, the minimally and non-minimally coupled scalar field models are obtaining good results to alleviate this tension [15, 16]. Furthermore, adding a scalar field in the dynamics of cosmology can give some scaling solutions [17–20]. These scaling solutions have a constant ratio between energy density of matter and the energy density corresponding to the scalar field, which is a good feature in the interest of solving the coincidence problem. Also, in comparison to the background density, the scalar field density is never neglected (even in the early time), therefore, the scalar field model is consistent with

the energy scale of particle physics [18]. Moreover, these scaling solutions can be attractors for different initial conditions and therefore, at the scaling regime, the cosmological dynamics is only depending on the theoretical parameters of the theory.

On the other hand, gravity can be describe in terms of curvature as in General Relativity (GR) or as general functions for scalar curvature,  $f(R)$  theories. Where, these  $f(R)$  theories are proposed for simplicity and for representing quantum corrections to GR [21–23]. And, the new terms for  $f(R)$  theories can be identified as an effective energy density and its corresponding pressure density for modified Friedmann equations and, consequently, these terms are recognized as dark energy [24, 25]. But, there is another possibility, gravity also can be described in terms of torsion, in which case, we have the Teleparallel Gravity (TG). In this theory, the dynamical variables are the tetrad field, instead of the usual metric tensor, and the Weitzenböck connection replaces the usual Levi-Civita connection [26–29]. This produces a conceptual change as a result of using torsion instead of curvature, even though the equations are the same. But this relation between curvature and torsion is only particular for the linear case, when we introduce modifications to gravity in the same way of  $f(R)$ , i.e. using a general function of the scalar torsion, we obtain the  $f(T)$  gravity. These theories are totally different, for example, the  $f(R)$  has field equations of fourth-order differential and  $f(T)$  has second-order equations, which is an advantage for this  $f(T)$  theory. And, if we add the fact that the  $f(T)$  theory can explain the accelerated expansion of our Universe, the observational solar system constrains [30–32], the cosmological perturbations [33, 34], etc. All this point out that  $f(T)$  is a good option to modify gravity. Even more, a generalization of  $f(T)$  is obtained by a non-minimal coupling between matter and torsion [34–36] when we consider a analogy to the non-minimal coupling between  $f(R)$  and matter, whose principal motivation are the counterterms that appear in quantizing a scalar field with self-interaction at curved spacetime [37]. On the other hand, a larger class of generalized teleparallel scalar-torsion  $f(T, \phi)$  gravity theories are necessary to generate primordial fluctuations during inflation [38] due to the non-minimal coupling between scalar field and a linear term of torsion cannot generate primordial fluctuations [39]. And, in the case of dark energy, theories with Lagrangian density  $f(T, \phi) = -T/2\kappa^2 - F(\phi)G(T) - V(\phi)$  are of interest considering that a non-minimal coupling between gravity and scalar field can provide scaling solutions [40, 41].

In this paper, we use a convenient set of dimensionless variables to study the dynamical system of background equations for a generalized teleparallel scalar-torsion  $f(T, \phi)$  gravity theory. Where, we choose a class of phenomenological model to analyse the new scaling solutions, the critical points and the respective stability conditions for the critical points. Also, we discuss the conditions to get a background consistent with the observational constraints at the present time. And we study the radiation, the matter and the dark energy dominated eras for the new solutions and the background cosmological dynamics. Finally, we summarize our findings and our conclusions.

## 2 Teleparallel Gravity

As a gauge theory for the translation group, Teleparallel Gravity (TG) constitutes an alternative description of gravity based on torsion [26–29]. And a distinctive characteristic is that the dynamical variable is the tetrad field  $e_A(x^\mu)$ , which connects the spacetime metric  $g_{\mu\nu}$

to the Minkowski tangent space metric  $\eta_{AB} = \text{diag}(-1, 1, 1, 1)$  using the local relation

$$g_{\mu\nu} = e^A{}_\mu e^B{}_\nu \eta_{AB}, \quad (2.1)$$

where  $e^A{}_\mu$  are the tetrad components in a coordinate base and also fulfilling the orthogonality conditions  $e^A{}_\mu e^{\nu A} = \delta^\nu_\mu$  and  $e^A{}_\mu e^{\mu B} = \delta^A_B$ , with  $e^{\mu B}$  the inverse components.

The action functional of TG is written as

$$S = -\frac{M_{pl}^2}{2} \int d^4x e T, \quad (2.2)$$

being  $T$  the torsion scalar,  $e = \det(e^A{}_\mu) = \sqrt{-g}$ , and  $M_{pl}^2 = (8\pi G)^{-1}$  the reduced Planck mass. Also, the torsion scalar is defined as

$$T = S_\rho{}^{\mu\nu} T^\rho{}_{\mu\nu}, \quad (2.3)$$

where

$$T^\rho{}_{\mu\nu} \equiv e_A{}^\rho [\partial_\mu e^A{}_\nu - \partial_\nu e^A{}_\mu + \omega^A{}_{B\mu} e^B{}_\nu - \omega^A{}_{B\nu} e^B{}_\mu], \quad (2.4)$$

are the components of torsion tensor, and

$$S_\rho{}^{\mu\nu} = \frac{1}{2} \left( K^{\mu\nu}{}_\rho + \delta^\mu_\rho T^{\theta\nu}{}_\theta - \delta^\nu_\rho T^{\theta\mu}{}_\theta \right), \quad (2.5)$$

is the so-called super-potential, with

$$K^{\mu\nu}{}_\rho = -\frac{1}{2} (T^{\mu\nu}{}_\rho - T^{\nu\mu}{}_\rho - T_\rho{}^{\mu\nu}). \quad (2.6)$$

the contorsion tensor.

The spin connection of TG is written as

$$\omega^A{}_{B\mu} = \Lambda^A{}_D(x) \partial_\mu \Lambda^D{}_B(x), \quad (2.7)$$

with  $\Lambda^A{}_D(x)$  like a local (point-dependent) Lorentz transformation [42]. And, as in the tetrad formalism for GR, it is necessary to introduce a Lorentz connection in order to ensure the covariance of the theory at hand [43]. Nonetheless, unlike the spin connection of GR, which is associated with both gravitational and inertial effects, the spin connection of TG represents only inertial effects of the frame [42]. Thus, there is a special class of inertial frames, called the proper frames in which it vanishes,  $\omega^A{}_{B\mu} = 0$ . Starting from this class of inertial frames we can get all the other classes of frames by performing local (point-dependent) Lorentz transformations on both, the tetrad and the spin connection [42].

The corresponding spacetime-indexed linear connection is

$$\Gamma^\rho{}_{\mu\nu} = e_A{}^\rho (\partial_\nu e^A{}_\mu + \omega^A{}_{B\nu} e^B{}_\mu), \quad (2.8)$$

which is the so-called Weitzenböck connection. It is related to the Levi-Civita connection of GR through

$$\Gamma^\rho{}_{\mu\nu} = \bar{\Gamma}^\rho{}_{\mu\nu} + K^\rho{}_{\mu\nu}. \quad (2.9)$$

Using this latter equation, it can be shown that

$$T = -R - e^{-1} \partial_\mu (e T^{\nu\mu}{}_\nu), \quad (2.10)$$

where  $R$  is the curvature scalar of Levi-Civita connection [42]. So, TG and GR are equivalent theories in the level of field equations.

At the moment of modifying gravity from the framework of TG, by introducing a non-minimally coupled matter field, as for example a scalar field [44–48], or putting into the action non-linear terms in the torsion scalar  $T$ , as for example in  $f(T)$  gravity [34, 49–51], it is obtained a new class of modified gravity theories with a rich phenomenology and not equivalent to their corresponding counterpart based on curvature [52].

### 3 Scalar-Torsion $f(T, \phi)$ Gravity

The relevant action is

$$S = \int d^4x e [f(T, \phi) + P(\phi)X] + S_m + S_r, \quad (3.1)$$

where  $f(T, \phi)$  is an arbitrary function of torsion scalar  $T$  and the scalar field  $\phi$  and  $X = -\partial_\mu\phi\partial^\mu\phi/2$ .  $S_m$  is the action of non-relativistic matter, including baryons and dark matter, and  $S_r$  is the action describing the radiation component.

Thus, we consider the flat Friedmann-Lemaître-Robertson-Walker (FLRW) universe with metric

$$ds^2 = -dt^2 + a^2 \delta_{ij} dx^i dx^j, \quad (3.2)$$

where  $a$  is the scale factor which is a function of the cosmic time  $t$ . Hence, the background equations are given by

$$f(T, \phi) - P(\phi)X - 2Tf_{,T} = \rho_m + \rho_r, \quad (3.3)$$

$$f(T, \phi) + P(\phi)X - 2Tf_{,T} - 4\dot{H}f_{,T} - 4H\dot{f}_{,T} = -p_r, \quad (3.4)$$

$$-P_{,\phi}X - 3P(\phi)H\dot{\phi} - P(\phi)\ddot{\phi} + f_{,\phi} = 0, \quad (3.5)$$

where  $H \equiv \dot{a}/a$  is the Hubble rate, a dot represents derivative with respect to  $t$ , and a comma denotes derivative with respect to  $\phi$  or  $X$ . Also, the functions  $\rho_i$ ,  $p_i$ , with  $i = m, r$  are the energy and pressure densities of non-relativistic matter (cold dark matter and baryons), and radiation, respectively, being that we already have used the corresponding barotropic equations of state  $w_m = p_m/\rho_m = 0$ , and  $w_r = p_r/\rho_r = 1/3$ , in the above equations.

In order to proceed forward we are going to consider the class of models with

$$f(T, \phi) = -\frac{1}{2\kappa^2}T - F(\phi)G(T) - V(\phi), \quad (3.6)$$

where  $V(\phi)$  is the scalar potential,  $F(\phi)$  the nonminimal coupling function of  $\phi$ , and  $G(T)$  an arbitrary function of  $T$ . Then, we obtain

$$\begin{aligned} \frac{3}{\kappa^2}H^2 &= G(T)F(\phi) - 2TG_{,T}F(\phi) + V + P(\phi)X \\ &\quad + \rho_m + \rho_r, \end{aligned} \quad (3.7)$$

$$\begin{aligned} -\frac{2}{\kappa^2}\dot{H} &= 2P(\phi)X + 4\dot{H}G_{,T}F(\phi) + 4HG_{,TT}\dot{T}F(\phi) \\ &\quad + 4HG_{,T}\dot{F} + \rho_m + \frac{4}{3}\rho_r, \end{aligned} \quad (3.8)$$

whereas the motion equation of  $\phi$  is written as

$$P(\phi)\ddot{\phi} + 3P(\phi)H\dot{\phi} + P_{,\phi}X + G(T)F_{,\phi} + V_{,\phi} = 0. \quad (3.9)$$

Following Ref. [53], the Friedmann equations (3.7) and (3.8) can also be rewritten as

$$\frac{3}{\kappa^2}H^2 = \rho_{de} + \rho_m + \rho_r, \quad (3.10)$$

$$-\frac{2}{\kappa^2}\dot{H} = \rho_{de} + p_{de} + \rho_m + \frac{4}{3}\rho_r, \quad (3.11)$$

where we have defined the energy and pressure densities of dark energy in the way

$$\rho_{de} = P(\phi)X + V - (2TG_{,T} - G)F(\phi), \quad (3.12)$$

$$p_{de} = P(\phi)X - V + (2TG_{,T} - G)F(\phi) + 4(2TG_{,TT} + G_{,T})F(\phi)\dot{H} + 4HG_{,T}F_{,\phi}\dot{\phi}. \quad (3.13)$$

Furthermore, we can define the effective dark energy equation-of-state parameter as

$$w_{de} = \frac{p_{de}}{\rho_{de}}. \quad (3.14)$$

One can easily see that  $\rho_{de}$  and  $p_{de}$  obey the standard evolution equation

$$\dot{\rho}_{de} + 3H(\rho_{de} + p_{de}) = 0. \quad (3.15)$$

which is consistent with energy conservation law and the fluid evolution equations

$$\dot{\rho}_m + 3H\rho_m = 0, \quad (3.16)$$

$$\dot{\rho}_r + 4H\rho_r = 0. \quad (3.17)$$

Lastly, concerning cosmological investigations it proves convenient to introduce the total equation-of-state parameter as

$$w_{tot} = \frac{p_{de} + p_r}{\rho_{de} + \rho_m + \rho_r}, \quad (3.18)$$

which is immediately related to the deceleration parameter  $q$  through

$$q = \frac{1}{2}(1 + 3w_{tot}), \quad (3.19)$$

and hence acceleration occurs when  $q < 0$ , as well as the standard density parameters

$$\Omega_m \equiv \frac{\kappa^2 \rho_m}{3H^2}, \quad \Omega_{de} \equiv \frac{\kappa^2 \rho_{de}}{3H^2}, \quad \Omega_r \equiv \frac{\kappa^2 \rho_r}{3H^2}, \quad (3.20)$$

such that

$$\Omega_{de} + \Omega_m + \Omega_r = 1. \quad (3.21)$$

In order to find cosmological solutions and to study the complete dynamics in the phase space for this class of dark energy models we are going to assume the ansatz

$$G(T) = \frac{T^{1+s}}{6^{1+s}}. \quad (3.22)$$

and  $P = 1$ . This non-linear coupling function in torsion is motivated from the physics of the very early universe, where it is associated with the generation of primordial fluctuations during inflation, in the context of  $f(T, \phi)$  gravity [38].

In this case, the energy and pressure densities of dark energy can be written as

$$\rho_{de} = \frac{\dot{\phi}^2}{2} + V - (1 + 2s)H^{2(1+s)}F(\phi), \quad (3.23)$$

$$\begin{aligned} p_{de} = & \frac{\dot{\phi}^2}{2} - V + (1 + 2s)H^{2(1+s)}F(\phi) \\ & + \frac{2}{3}(1 + s)(1 + 2s)H^{2s}F(\phi)\dot{H} \\ & + \frac{2}{3}(1 + s)H^{1+2s}F_{,\phi}\dot{\phi}, \end{aligned} \quad (3.24)$$

and the motion equation of  $\phi$  becomes

$$\ddot{\phi} + 3H\dot{\phi} + H^{2(1+s)}F_{,\phi} + V_{,\phi} = 0. \quad (3.25)$$

Thus, Eqs. (3.10), (3.11), along with equations (3.23), (3.24), and Eqs. (3.16), (3.17), and (3.25), compose the set of cosmological equations for the model.

## 4 Dynamical system

To obtain the corresponding autonomous system associated with the above set of cosmological equations of the model, we introduce the following useful dimensionless variables [53, 54]

$$\begin{aligned} x &= \frac{\kappa\dot{\phi}}{\sqrt{6}H}, \quad y = \frac{\kappa\sqrt{V}}{\sqrt{3}H}, \\ z &= -\frac{1}{3}(2s + 1)F(\phi)H^{2s}, \quad \varrho = \frac{\sqrt{\rho_r}}{\sqrt{3}H}, \end{aligned} \quad (4.1)$$

and,

$$\lambda = -\frac{V'(\phi)}{V(\phi)}, \quad \sigma = -\frac{F'(\phi)}{F(\phi)}, \quad (4.2)$$

$$\Gamma = \frac{V(\phi)V''(\phi)}{V'(\phi)^2}, \quad \Theta = \frac{F(\phi)F''(\phi)}{F'(\phi)^2}, \quad (4.3)$$

then, the constraint equation

$$x^2 + y^2 + z + \Omega_m + \varrho^2 = 1. \quad (4.4)$$

Therefore, we obtain the dynamical system

$$\frac{dx}{dN} = \frac{-f_1(x, y, z, \varrho)}{2(1+2s)[(s+1)z-1]}, \quad (4.5)$$

$$\frac{dy}{dN} = \frac{-yf_2(x, y, z, \varrho)}{2(1+2s)[(s+1)z-1]}, \quad (4.6)$$

$$\frac{dz}{dN} = \frac{zf_3(x, y, z, \varrho)}{(1+2s)[(s+1)z-1]}, \quad (4.7)$$

$$\frac{d\varrho}{dN} = \frac{-\varrho f_4(x, y, z, \varrho)}{2(1+2s)[(s+1)z-1]}, \quad (4.8)$$

$$\frac{d\lambda}{dN} = -\sqrt{6}(\Gamma-1)\lambda^2 x, \quad (4.9)$$

$$\frac{d\sigma}{dN} = -\sqrt{6}(\Theta-1)\sigma^2 x, \quad (4.10)$$

where we have defined

$$\begin{aligned} f_1(x, y, z, \varrho) = & (6s+3)x^3 + 2\sqrt{6}(s+1)\sigma x^2 z + \\ & (2s+1)x[(6s+3)z - 3y^2 + \varrho^2 - 3] + \\ & \sqrt{6}[(s+1)z-1][\sigma z - y^2(\lambda + 2\lambda s)], \end{aligned} \quad (4.11)$$

$$\begin{aligned} f_2(x, y, z, \varrho) = & \sqrt{6}x[(s+1)z(\lambda + 2\lambda s + 2\sigma) - \lambda(2s+1)] - \\ & (2s+1)[3(y^2 + z - 1) - \varrho^2] + (6s+3)x^2, \end{aligned} \quad (4.12)$$

$$\begin{aligned} f_3(x, y, z, \varrho) = & 3s(2s+1)x^2 - \sqrt{6}\sigma x[(s+1)z - 2s - 1] + \\ & s(2s+1)[\varrho^2 - 3(y^2 + z - 1)], \end{aligned} \quad (4.13)$$

$$\begin{aligned} f_4(x, y, z, \varrho) = & (6s+3)x^2 + 2\sqrt{6}(s+1)\sigma x z + \\ & (2s+1)(4sz - 3y^2 + z + \varrho^2 - 1). \end{aligned} \quad (4.14)$$

Using the above set of phase space variables we also can write

$$\Omega_{de} = x^2 + y^2 + z, \quad \Omega_m = 1 - x^2 - y^2 - z, \quad \Omega_r = \varrho^2. \quad (4.15)$$

Similarly, the equation of state of dark energy  $w_{de} = p_{de}/\rho_{de}$  can be rewritten as

$$\begin{aligned} w_{de} = & \frac{2\sqrt{\frac{2}{3}}\sigma x z}{(z-2)(sz+z-1)(x^2+y^2+z)} - \\ & \frac{\frac{2\sqrt{6}\sigma x z}{(2s+1)(z-2)} + \varrho^2 + 3}{3(x^2+y^2+z)} - \frac{3x^2 - 3(y^2 + z - 1) + \varrho^2}{3[z(s+1) - 1](x^2+y^2+z)}, \end{aligned} \quad (4.16)$$

whereas the total equation of state becomes

$$w_T = -1 + \frac{1}{s+1} + \frac{(s+1)(y^2 - x^2) - s}{(s+1)[z(s+1) - 1]} + \quad (4.17)$$

$$\frac{4\sqrt{\frac{2}{3}}\sigma x}{(2s+1)(z-2)} - \frac{(2s+1)\varrho^2 + 2\sqrt{6}\sigma x}{3(2s+1)[(s+1)z - 1]} - \frac{2\sqrt{\frac{2}{3}}\sigma x z}{(2s+1)(z-2)}. \quad (4.18)$$

The dynamical system (4.5)-(4.10) is not an autonomous system unless the parameters  $\Gamma$  and  $\Theta$  are known [53, 54]. From now we concentrate in the exponential potential  $V(\phi) = V_0 e^{-\lambda\kappa\phi}$ , with  $\lambda$  a dimensionless constant, that is,  $\Gamma = 1$ . Let us remember that this scalar potential can give rise to an accelerated expansion and to the same time allows to obtain cosmological scaling solutions [24, 53]. On the other hand, for the nonminimal coupling function of  $\phi$  we take  $F(\phi) = F_0 e^{-\sigma\kappa\phi}$ , such that  $\Theta = 1$ . This is the most natural and simple choice for the nonminimal coupling function compatible with the exponential scalar potential [41].

## 5 Critical Points

We obtain the critical points or fixed points  $(x_c, y_c, z_c, \varrho_c)$  of the corresponding autonomous system by imposing the conditions  $dx/dN = dy/dN = dz/dN = d\varrho/dN = 0$ . From the definition (4.1), the values  $x_c, y_c, z_c$  and  $\varrho_c$  must be reals with  $y_c \geq 0$  and  $\varrho_c \geq 0$ . The critical points are presented in the Table 1, while the expressions for the cosmological parameters for each critical point are shown in Table 2.

The point  $a_R$  is a radiation-dominated solution  $\Omega_r = 1$  with a total equation of state  $w_{tot} = 1/3$ . The equation of state of dark energy takes the value  $w_{de} = (4s+1)/3$ , which depends on the parameter  $s$ . It exist for all the values of parameters  $s, \sigma$  and  $\lambda$ . Point  $b_R$  is a scaling solution with  $\Omega_{de}^{(r)} = 4/\lambda^2$ , and  $\Omega_m = 0$ . For this point we found  $w_{de} = w_{tot} = 1/3$ . The physical condition  $0 < \Omega_{de}^{(r)} < 1$  imposes the constraint  $|\lambda| > 2$ . Point  $c_R$  is also a scaling solution which is a new solution that exist only for  $s \neq 0$ . The fractional energy density parameter of dark energy is  $\Omega_{de}^{(r)} = 4s(4s+1)/(3\sigma^2)$ , and  $\Omega_m = 0$ . The constraints for the parameters due to the physical condition  $0 < \Omega_{de}^{(r)} < 1$  have been put in Table 3. This point also satisfies  $w_{de} = w_{tot} = 1/3$ . So, points  $b_R$  and  $c_R$  describe a non-standard radiation-dominated era in which there is a small contribution coming from dark energy. Thus, if  $b_R$  and  $c_R$  are both responsible for the scaling radiation era we need also to consider the earliest constraint coming from physics of big bang nucleosynthesis (BBN) which requires  $\Omega_{de}^{(r)} < 0.045$  [55, 56]. So, in the case of point  $b_R$  we find  $|\lambda| > 9.94$ , while for  $c_R$  we obtain  $-0.25 < s \leq 0$  for  $\sigma \neq 0$ , or,  $s \leq -0.25$  (or  $s > 0$ ) and  $|\sigma| > 5.44\sqrt{s(4s+1)}$ .

Point  $d_M$  represents a standard cold dark matter-dominated era with  $\Omega_m = 1$ ,  $\omega_{de} = s$  and  $w_{tot} = 0$ . This point exists for all the values of parameters. Points  $e, f$  satisfy  $\Omega_{de} = 1$ , but they cannot explain the current accelerated expansion because them behave as stiff matter with  $w_{de} = w_{tot} = 1$ . On the other hand, point  $g_M$  describes a non-standard cold dark matter-dominated era with a small contribution of the fractional dark energy density parameter given by  $\Omega_{de}^{(m)} = 3/\lambda^2$ ,  $\Omega_r = 0$ , and  $w_{de} = w_{tot} = 0$ . The point  $i_M$  is a new fixed point which is present only for  $s \neq 0$  and it is a scaling solution representing a non-standard

**Table 1.** Critical points for the autonomous system (4.5)-(4.10) for  $V(\phi) = V_0 e^{-\lambda\kappa\phi}$  and  $F(\phi) = F_0 e^{-\sigma\kappa\phi}$ . We have defined  $A = 9s^2(2s+1)^2 - 6s(s+1)\sigma^2$ .

Name	$x_c$	$y_c$	$z_c$	$q_c$
$a_R$	0	0	0	1
$b_R$	$\frac{2\sqrt{\frac{2}{3}}}{\lambda}$	$\frac{2}{\sqrt{3}\lambda}$	0	$\sqrt{1 - \frac{4}{\lambda^2}}$
$c_R$	$-\frac{2\sqrt{\frac{2}{3}}s}{\sigma}$	0	$\frac{4s(2s+1)}{3\sigma^2}$	$\sqrt{1 - \frac{4s(4s+1)}{3\sigma^2}}$
$d_M$	0	0	0	0
$e$	-1	0	0	0
$f$	1	0	0	0
$g_M$	$\frac{\sqrt{\frac{3}{2}}}{\lambda}$	$\sqrt{\frac{3}{2}}\sqrt{\frac{1}{\lambda^2}}$	0	0
$h$	$\frac{\lambda}{\sqrt{6}}$	$\sqrt{1 - \frac{\lambda^2}{6}}$	0	0
$i_M$	$-\frac{\sqrt{\frac{3}{2}}s}{\sigma}$	0	$\frac{3s(2s+1)}{2\sigma^2}$	0
$j$	$-\frac{3s(2s+1)+\sqrt{A}}{\sqrt{6}(s+1)\sigma}$	0	$\frac{(2s+1)(3s(x_c^2+1)+\sqrt{6}\sigma x_c)}{\sqrt{6}(s+1)\sigma x_c+3s(2s+1)}$	0
$k$	$\frac{-3s(2s+1)+\sqrt{A}}{\sqrt{6}(s+1)\sigma}$	0	$\frac{(2s+1)(3s(x_c^2+1)+\sqrt{6}\sigma x_c)}{\sqrt{6}(s+1)\sigma x_c+3s(2s+1)}$	0
$l$	0	$\sqrt{\frac{\sigma}{(2s+1)(\lambda+\frac{\sigma}{2s+1})}}$	$\frac{\lambda(2s+1)}{\lambda+2\lambda s+\sigma}$	0

cold dark matter-dominated era with  $\Omega_{de}^{(m)} = 3s(3s+1)/(2\sigma^2)$ ,  $\Omega_r = 0$ , and  $w_{de} = w_{tot} = 0$ . The constraints for the parameters obtained from the physical condition  $0 < \Omega_{de}^{(m)} < 1$  are shown in Table 3. If points  $g_M$  and  $i_M$  represent both the scaling matter era they are constrained to satisfy  $\Omega_{de}^{(m)} < 0.02$  (95% C.L.), at redshift  $z \approx 50$ , according to CMB measurements [57]. Thus, for  $g_M$  we find  $|\lambda| > 12.25$ , while for  $i_M$  we get  $-0.3 < s \leq 0$  for  $\sigma \neq 0$ , or  $s \leq -0.3$  (or  $s > 0$ ) and  $|\sigma| > \sqrt{s(225s+75)}$ .

Point  $h$  is identified as dark energy-dominated era with  $\Omega_{de} = 1$ , and  $w_{de} = w_{tot} = (\lambda^2 - 3)/3$ . It exists for  $|\lambda| < \sqrt{6}$  and it can explain the current cosmic acceleration for  $|\lambda| < \sqrt{2}$  [53]. Points  $j$  and  $k$  provide dark energy-dominated eras which can explain the cosmic accelerated expansion. These are also new solutions of dark energy which are present only for  $s \neq 0$ . The expressions for  $w_{de}$  and  $w_{tot}$  are shown in Table 2, whereas the existence and accelerated expansion conditions are detailed in Table 3. Finally, point  $l$  is a de Sitter solution with  $\Omega_{de} = 1$ , and  $w_{de} = w_{tot} = -1$ , which provides accelerated expansion for the all values of the parameters. Although this points exist for  $s = 0$ , the new expression for the phase space coordinated  $y_c$  associated with it and reported in Table 1 is a generalisation of the case  $s = 0$ , which now also includes values for  $s \neq 0$ . The conditions of existence for this point have also been detailed in Table 3.

**Table 2.** Cosmological parameters for the critical points in Table 1. We have define  $A = 9s^2(2s + 1)^2 - 6s(s + 1)\sigma^2$ . The fractional energy density of the radiation fluid is calculated through  $\Omega_r = \varrho^2 = 1 - \Omega_m - \Omega_{de}$ .

Name	$\Omega_{de}$	$\Omega_m$	$\omega_{de}$	$\omega_{tot}$
$a_R$	0	0	$\frac{1}{3}(4s + 1)$	$\frac{1}{3}$
$b_R$	$\frac{4}{\lambda^2}$	0	$\frac{1}{3}$	$\frac{1}{3}$
$c_R$	$\frac{4s(4s+1)}{3\sigma^2}$	0	$\frac{1}{3}$	$\frac{1}{3}$
$d_M$	0	1	$s$	0
$e$	1	0	1	1
$f$	1	0	1	1
$g_M$	$\frac{3}{\lambda^2}$	$1 - \frac{3}{\lambda^2}$	0	0
$h$	1	0	$\frac{1}{3}(\lambda^2 - 3)$	$\frac{1}{3}(\lambda^2 - 3)$
$i_M$	$\frac{3s(3s+1)}{2\sigma^2}$	$1 - \frac{3s(3s+1)}{2\sigma^2}$	0	0
$j$	1	0	$\frac{\sqrt{A+3s^2}}{3s(s+1)}$	$\frac{\sqrt{A+3s^2}}{3s(s+1)}$
$k$	1	0	$\frac{3s^2 - \sqrt{A}}{3s(s+1)}$	$\frac{3s^2 - \sqrt{A}}{3s(s+1)}$
$l$	1	0	-1	-1

## 6 Stability of critical points

In order to study the stability of the critical points we consider time dependent liner perturbations  $\delta x$ ,  $\delta y$ ,  $\delta z$  and  $\delta \varrho$  around each critical point in the form  $x = x_c + \delta x$ ,  $y = y_c + \delta y$ ,  $z = z_c + \delta z$ , and  $\varrho = \varrho_c + \delta \varrho$ . By substituting these expressions into the autonomous system (4.5)-(4.9) and linearising them we obtain the linear perturbation matrix  $\mathcal{M}$  [53]. The eigenvalues of  $\mathcal{M}$ , namely,  $\mu_1$ ,  $\mu_2$ ,  $\mu_3$  and  $\mu_4$  evaluated at each fixed point determines the stability conditions for each one of them. The classification of the stability properties is established usually in the following way: (i) Stable node: all the eigenvalues are negative; (ii) Unstable node: all the eigenvalues are positive; (iii) Saddle point: one or three of the four eigenvalues are positive and the others are negative; (iv) Stable spiral: The determinant of  $\mathcal{M}$  is negative, and the real part of all the eigenvalues are negative. Points which are stable node or stable spiral are called attractor points, and these fixed points are reached through the cosmological evolution of the Universe, independently of the initial conditions. The conditions of existence, stability and acceleration of critical points for system (4.5)-(4.9) are shown in Table 3.

- Point  $a_R$  has the eigenvalues

$$\mu_1 = -1, \quad \mu_2 = 1, \quad \mu_3 = 2, \quad \mu_4 = -4s, \quad (6.1)$$

then this point is always a saddle point.

- For point  $b_R$  we obtain

$$\mu_1 = 1, \quad \mu_{2,3} = \frac{1}{2} \left( -1 \mp \sqrt{\frac{64}{\lambda^2} - 15} \right), \quad \mu_4 = -\frac{4(\lambda s + \sigma)}{\lambda}, \quad (6.2)$$

that it is a saddle point for all the values of parameters.

- Similarly, point  $c_R$  has the eigenvalues

$$\mu_1 = 1, \quad \mu_2 = \frac{2\lambda s}{\sigma} + 2, \quad \mu_{3,4} = -\frac{1}{2} \mp \sqrt{\frac{4s[4s(4s+1) - 3\sigma^2]}{4s(s+1)(2s+1) - 3\sigma^2} + \frac{1}{4}}, \quad (6.3)$$

and it is also always a saddle point.

- Point  $d_M$  leads us to

$$\mu_1 = -\frac{1}{2}, \quad \mu_2 = -\frac{3}{2}, \quad \mu_3 = \frac{3}{2}, \quad \mu_4 = -3s. \quad (6.4)$$

that it is always a saddle point.

- For points  $e$  and  $f$  we find

$$\mu_1 = 3, \quad \mu_2 = 1, \quad \mu_3 = 3 \pm \sqrt{\frac{3}{2}}\lambda, \quad \mu_4 = -6s \pm \sqrt{6}\sigma, \quad (6.5)$$

where (+) corresponds to  $e$  and (-) to  $f$ . Point  $e$  is an unstable node for  $s < \frac{\sigma}{\sqrt{6}}$  and  $\lambda > -\sqrt{6}$  with  $\sigma \in \mathbb{R}$ . In any other case it is a saddle point. Also, point  $f$  is an unstable node for  $\lambda < \sqrt{6}$  and  $s < -\frac{\sigma}{\sqrt{6}}$ , with  $\sigma \in \mathbb{R}$ . If one of these conditions is not satisfied it is a saddle point.

- Point  $g_M$  has associated the eigenvalues

$$\mu_1 = -\frac{1}{2}, \quad \mu_{2,3} = \frac{3}{4} \left( -1 \mp \sqrt{\frac{24}{\lambda^2} - 7} \right), \quad \mu_4 = -\frac{3(\lambda s + \sigma)}{\lambda}, \quad (6.6)$$

that it is a saddle point for  $-2\sqrt{\frac{6}{7}} \leq \lambda < -\sqrt{3}$  and  $\sigma > -\lambda s$ , or  $\sqrt{3} < \lambda \leq 2\sqrt{\frac{6}{7}}$  and  $\sigma < -\lambda s$ , with  $s \in \mathbb{R}$ . On the other hand, it is a stable node for  $s \in \mathbb{R}$ , and,  $-2\sqrt{\frac{6}{7}} < \lambda < -\sqrt{3} \wedge \sigma < -\lambda s$ , or  $\sqrt{3} < \lambda < 2\sqrt{\frac{6}{7}} \wedge \sigma > -\lambda s$ . However, this point cannot provide the current accelerated expansion of Universe.

- For point  $h$  we get

$$\mu_1 = \frac{1}{2}(\lambda^2 - 6), \quad \mu_2 = \frac{1}{2}(\lambda^2 - 4), \quad \mu_3 = \lambda^2 - 3, \quad \mu_4 = -\lambda(\lambda s + \sigma). \quad (6.7)$$

This critical point has a range in the space of values of parameters with accelerated expansion and we are interested in its stability conditions within this range. One finds that when point  $h$  has accelerated expansion it is a stable node for  $-\sqrt{2} < \lambda < 0 \wedge \sigma < -\lambda s$ , or  $0 < \lambda < \sqrt{2} \wedge \sigma > -\lambda s$ , with  $s \in \mathbb{R}$ , and other case it is a saddle point.

- In the case of point  $i_M$  one finds

$$\mu_1 = -\frac{1}{2}, \quad \mu_2 = \frac{3(\lambda s + \sigma)}{2\sigma}, \quad \mu_{3,4} = 3 \left( -\frac{1}{4} \mp \sqrt{-\frac{3s^4}{3s(s+1)(2s+1) - 2\sigma^2} + \frac{s}{2} + \frac{1}{16}} \right). \quad (6.8)$$

Since it is a matter solution we are interested for which region of parameters it is unstable. When it is unstable it is always a saddle point and the corresponding region of parameters has been put in Table 3. This scaling solution can also be a stable node for some region of parameters, as for example for  $s > 0 \wedge -\sqrt{3} \sqrt{\frac{s(s(26s+11)+1)}{16s+2}} < \sigma < -\sqrt{\frac{3}{2}} \sqrt{s(3s+1)} \wedge \lambda > -\frac{\sigma}{s}$ . Nonetheless, it is not viable to explain a late-time acceleration.

- Also, for points  $j$  and  $k$  we obtain

$$\begin{aligned} \mu_1 &= \frac{[3s(2s+1) \pm \sqrt{A}](\lambda s + \sigma)}{2s(s+1)\sigma}, \quad \mu_2 = \frac{-3s \pm \sqrt{A}}{2s(s+1)}, \quad \mu_3 = \frac{s(2s-1) \pm \sqrt{A}}{2s(s+1)}, \\ \mu_4 &= \frac{3s^2 \pm \sqrt{A}}{s(s+1)}, \end{aligned} \quad (6.9)$$

where  $A = 9s^2(2s+1)^2 - 6s(s+1)\sigma^2$ , and sign (+) is for  $j$ , and (-) for  $k$ . Both points are dark energy solutions which can explain the current accelerated expansion of the Universe. Therefore we are interested in to find the stability conditions for these points when they provide accelerated expansion. From the above eigenvalues we find that exist a region of the space of parameters in which these points are stable nodes and thus attractors. These constraints for the parameters are shown in Table 3.

- Finally, for point  $l$  we find the eigenvalues

$$\mu_1 = -2, \quad \mu_2 = -3, \quad \mu_{3,4} = -\frac{3}{2} \mp \sqrt{\frac{9}{4} - \frac{3\lambda\sigma(\lambda s + \sigma)}{\lambda s(2s+1) - \sigma}}. \quad (6.10)$$

This is a de Sitter solution which therefore provides accelerated expansion for all the values of the parameters. We find it is a stable node for  $\lambda > 0 \wedge s > 0 \wedge 0 < \sigma \leq \left[ -4\lambda^2 s + \lambda \sqrt{\frac{9}{\lambda^2} + 8s(2(\lambda^2 + 6)s + 9)} - 3 \right] / (8\lambda)$ . Also, for  $s < 0$  this point can be a stable node under some constraints of the parameters  $s$ ,  $\lambda$  and  $\sigma$ , but the expressions for these constraints are some complicated and we do not put them explicitly here. Never this point is a stable spiral.

**Table 3.** Properties of critical points.

Name	Existence	Stability	Acceleration
$a_R$	$\forall s, \lambda, \sigma$	unstable $\forall s, \lambda, \sigma$	never
$b_R$	$ \lambda  > 2$	unstable $\forall s, \lambda, \sigma$	never
$c_R$	$\sigma \neq 0$	unstable $\forall s, \lambda, \sigma$	never
	$\wedge(-\frac{1}{8}\sqrt{12\sigma^2+1}-\frac{1}{8} < s < -\frac{1}{4})$	unstable $\forall s, \lambda, \sigma$	never
	$\vee(0 < s < \frac{1}{8}\sqrt{12\sigma^2+1}-\frac{1}{8})$	unstable $\forall s, \lambda, \sigma$	never
$d_M$	$\forall s, \lambda, \sigma$	unstable $\forall s, \lambda, \sigma$	never
$e$	$\forall s, \lambda, \sigma$	unstable $\forall s, \lambda, \sigma$	never
$f$	$\forall s, \lambda, \sigma$	unstable $\forall s, \lambda, \sigma$	never
$g_M$	$ \lambda  > \sqrt{3}$	unstable for $s \in \mathbb{R}$	never
		$\wedge(\lambda < -\sqrt{3} \wedge \sigma > -\lambda s)$	
		$\vee(\lambda > \sqrt{3} \wedge \sigma < -\lambda s)$	
$h$	$ \lambda  < \sqrt{6}$	$s \in \mathbb{R}$	$ \lambda  < \sqrt{2}$
		$\wedge(-\sqrt{2} < \lambda < 0 \wedge \sigma < -\lambda s)$	
		$\vee(0 < \lambda < \sqrt{2} \wedge \sigma > -\lambda s)$	
$i_M$	$s > 0 \wedge  \sigma  > \sqrt{\frac{3s(3s+1)}{2}}$	unstable for	never
	$s < -\frac{1}{3} \wedge  \sigma  > \sqrt{\frac{3s(3s+1)}{2}}$	$s > 0 \wedge  \sigma  > \sqrt{\frac{3s(s+1)(2s+1)}{2}}$	
		$-\frac{1}{6}\sqrt{8\sigma^2+1}-\frac{1}{6} < s < -\frac{1}{3}$	
		$\wedge(\sigma > 0 \wedge \lambda < -\frac{\sigma}{s})$	
		$\vee(\sigma < 0 \wedge \lambda > -\frac{\sigma}{s})$	
$j$	$s > 0 \wedge  \sigma  \leq \sqrt{\frac{3s(2s+1)^2}{2(s+1)}}$	$-1 < s < 0$	$\sigma \in \mathbb{R} \wedge -1 < s < 0$
	$s < -1 \wedge  \sigma  \leq \sqrt{\frac{3s(2s+1)^2}{2(s+1)}}$	$\wedge(\lambda \leq 0 \wedge (\sigma < -\lambda s \vee \sigma > 0))$	
	$-1 \leq s < 0$ and $\sigma \in \mathbb{R}$	$\vee(\lambda > 0 \wedge (\sigma < 0 \vee \sigma > -\lambda s))$	
$k$	$s > 0 \wedge  \sigma  \leq \sqrt{\frac{3s(2s+1)^2}{2(s+1)}}$	$s > \sqrt{\frac{3\sigma^2}{10} + \frac{1}{25}} - \frac{1}{5}$	$ \sigma  < \sqrt{\frac{2s(5s+2)}{3}}$
	$s < -1 \wedge  \sigma  \leq \sqrt{\frac{3s(2s+1)^2}{2(s+1)}}$	$\wedge(\sigma < 0 \wedge \lambda > -\frac{\sigma}{s})$	$\wedge s > 0$
	$-1 \leq s < 0$ and $\sigma \in \mathbb{R}$	$\vee(\sigma > 0 \wedge \lambda < -\frac{\sigma}{s})$	$\vee(-1 < s < -\frac{2}{5} \vee s < -1)$
		$s < -\sqrt{\frac{3\sigma^2}{10} + \frac{1}{25}} - \frac{1}{5}$	
		$\wedge(\sigma \leq -\sqrt{2} \wedge \lambda < -\frac{\sigma}{s})$	
		$\vee(\sigma > \sqrt{2} \wedge \lambda > -\frac{\sigma}{s})$	
		$s < -1$	
		$\wedge(-\sqrt{2} < \sigma < 0 \wedge \lambda < -\frac{\sigma}{s})$	
		$\vee(0 < \sigma \leq \sqrt{2} \wedge \lambda > -\frac{\sigma}{s})$	
		$-1 < s < -\sqrt{\frac{3\sigma^2}{10} + \frac{1}{25}} - \frac{1}{5}$	
		$\wedge(-\sqrt{2} < \sigma < 0 \wedge \lambda < -\frac{\sigma}{s})$	
		$\vee(0 < \sigma < \sqrt{2} \wedge \lambda > -\frac{\sigma}{s})$	
$l$	$\sigma < 0 \wedge s > 0 \wedge \lambda < -\frac{\sigma}{2s+1}$	$\lambda > 0 \wedge s > 0 \wedge$	always
	$\sigma > 0 \wedge s > 0 \wedge \lambda > -\frac{\sigma}{2s+1}$	$0 < \sigma \leq \frac{-4\lambda^2 s + \lambda \sqrt{\frac{9}{\lambda^2} + 8s(2(\lambda^2+6)s+9)} - 3}{8\lambda}$	
	$\sigma < 0 \wedge s < -\frac{1}{2} \wedge \lambda > -\frac{\sigma}{2s+1}$		
	$\sigma > 0 \wedge s < -\frac{1}{2} \wedge \lambda < -\frac{\sigma}{2s+1}$		
	$\sigma < 0 \wedge -\frac{1}{2} < s < 0 \wedge \lambda < -\frac{\sigma}{2s+1}$		
	$\sigma > 0 \wedge -\frac{1}{2} < s < 0 \wedge \lambda > -\frac{\sigma}{2s+1}$		

## 7 Numerical results

We have found four final attractors which represent the dark energy dominated epoch with cosmic acceleration, the points  $h$ ,  $k$ ,  $j$  and  $l$ . The attractor  $h$  is already present in the ordinary minimally coupled exponential quintessence model [24], but,  $k$ ,  $j$ , and  $l$  are new solutions which only arise in the nonminimal case and for  $s \neq 0$ . Furthermore, it is found the scaling solutions  $b_R$ ,  $c_R$  which are saddle points and represent the scaling radiation era, being that  $c_R$  is a new scaling solution only present in the nonminimal case and for  $s \neq 0$ , and also, the scaling solutions  $g_M$  and  $i_M$  which are saddle points representing the scaling

dark matter era, with  $i_M$  also only present in the nonminimal case and  $s \neq 0$ .

In FIGS. 1, 2, and 3, we show the phase space trajectories  $a_R \rightarrow d_M \rightarrow k$ ,  $a_R \rightarrow g_M \rightarrow k$  and  $b_R \rightarrow g_M \rightarrow k$ . In FIG. 1 we depict the behaviour of the energy densities of dark energy, dark matter and radiation, while in FIG. 2 we show the total equation of state and the equation of state of dark energy. The time of radiation-matter equality is around  $z \approx 3.387$ , the transition to the accelerated phase happens at  $z \approx 0.22$ , very close to  $\Lambda$ CDM value, and it is obtained the current values of the fractional energy density parameters of dark energy  $\Omega_{de}^{(0)} \approx 0.68$  and dark matter  $\Omega_m^{(0)} \approx 0.32$ , with the equation of state of dark energy given by  $w_{de}(z=0) \approx -1.05$ , which is consistent with the observational constraint  $w_{de}^{(0)} = -1.028 \pm 0.032$ , and the other constraints for the cosmological parameters from Planck [3]. Additionally, during the radiation and dark matter scaling regimes, for the evolution curves  $a_R \rightarrow g_M \rightarrow k$ , and  $b_R \rightarrow g_M \rightarrow k$ , we have applied the constraints on the fractional energy density parameters of dark energy,  $\Omega_{de}^{(r)}$ ,  $\Omega_{de}^{(m)}$ , coming from the Physics of Big Bang Nucleosynthesis (BBN),  $\Omega_{de}^{(r)} < 0.045$  [56], and CMB measurements from Planck,  $\Omega_{de}^{(m)} < 0.02$  (95% CL), at redshift  $z \approx 50$  [57]. For example, in FIG 1, during the scaling radiation era  $b_R$ , we obtain  $\Omega_{de}^{(r)} \approx 2 \times 10^{-4}$ , and during the scaling matter era  $g_M$ , we find  $\Omega_{de}^{(m)} = 1.37 \times 10^{-4}$  (dashed blue line),  $\Omega_{de}^{(m)} = 1.88 \times 10^{-6}$  (dot-dashed blue line), and  $\Omega_{de}^{(m)} = 1.36 \times 10^{-4}$  (solid blue line), at redshift  $z = 50$ .

Similarly, in FIGS. 4, 5, and 6, we show the evolution curves in the phase space for the transitions  $a_R \rightarrow d_M \rightarrow h$ ,  $a_R \rightarrow i_M \rightarrow h$  and  $c_R \rightarrow i_M \rightarrow h$ . In FIGS. 4, and 5, we plot the evolution of the energy densities of the matter components and the total equation of state and the equation of state of dark energy, respectively. As before, the redshift of radiation-matter equality is around  $z \approx 3.387$ , and the transition to the accelerated phase at  $z \approx 0.22$ , very close to  $\Lambda$ CDM value. Also, these evolution trajectories can adjust the current values of the fractional energy density parameters of dark energy  $\Omega_{de}^{(0)} \approx 0.68$  and dark matter  $\Omega_m^{(0)} \approx 0.32$ , and the equation of state of dark energy now takes the value  $w_{de}(z=0) = -0.997$ , which is again consistent with observational constraints from Planck [3]. Likewise, during the scaling radiation era represented by the critical point  $c_R$ , we have  $\Omega_{de}^{(r)} = 0.008$ , which is consistent with the BBN constraint [56], and for the scaling matter  $i_M$  we get  $\Omega_{de}^{(m)} = 1.59 \times 10^{-5}$  (dashed blue line),  $\Omega_{de}^{(m)} = 5.89 \times 10^{-3}$  (solid blue line), and  $\Omega_{de}^{(m)} = 5.85 \times 10^{-3}$  (dot-dashed blue line), at  $z = 50$ , which is also consistent with CMB measurements [57].

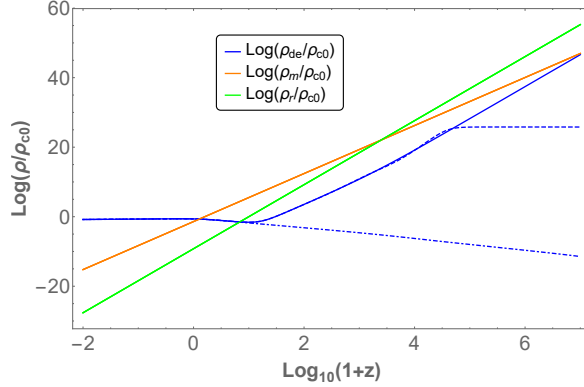


**Figure 1.** We depict the evolution of the energy density of dark energy  $\rho_{de}$  (blue), dark matter (including baryons)  $\rho_m$  (orange) and radiation  $\rho_r$  (green) as functions of the redshift  $z$ , for  $s = -1.20$ ,  $\sigma = 0.3$  and  $\lambda = 150$ . The solid blue line corresponds to the initial conditions  $x_i = 0.0108$ ,  $y_i = 0.00765$ ,  $z_i = 9.3 \times 10^{-30}$ ,  $\varrho_i = 0.999788$ , dashed blue line to  $x_i = 1 \times 10^{-9}$ ,  $y_i = 4 \times 10^{-7}$ ,  $z_i = 9.1 \times 10^{-30}$ ,  $\varrho_i = 0.999877$ , and dot-dashed blue line to  $x_i = 1 \times 10^{-33}$ ,  $y_i = 1 \times 10^{-41}$ ,  $z_i = 1.05 \times 10^{-29}$ ,  $\varrho_i = 0.999877$ . It is observed the two new scaling regimes during the radiation and dark matter era. To obtain this plot we have found the current values for the fractional energy densities of dark energy  $\Omega_{de}^{(0)} = 0.68$  and dark matter  $\Omega_m^{(0)} = 0.32$ , at redshift  $z = 0$ , according to Planck results [3]. Also, during the scaling radiation epoch we have imposed the BBN constraint  $\Omega_{de}^{(r)} < 0.045$  [56], and the constraint for the field energy density during the scaling matter epoch  $\Omega_{de}^{(m)} < 0.02$  (95% C.L.), at redshift  $z \approx 50$ , from CMB measurements [57].

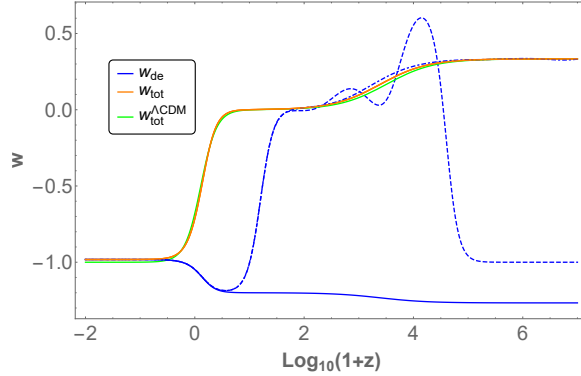


**Figure 2.** It is shown the behaviour of the total equation of state  $w_{tot}$  (orange line), the equation of state of dark energy  $w_{de}$  (blue line), and the total equation of state of  $\Lambda$ CDM model (green line) as functions of the redshift  $z$ , for the values of parameters for  $s = -1.20$ ,  $\sigma = 0.3$  and  $\lambda = 150$ . Also, for solid, dashed, and dot-dashed blue lines we have the same initial conditions of FIG. 1. It is observed the phantom value  $w_{de} \approx -1.05$  at the current time  $z = 0$ , which is consistent with the observational constraint  $w_{de}^{(0)} = -1.028 \pm 0.032$ , from Planck [3].

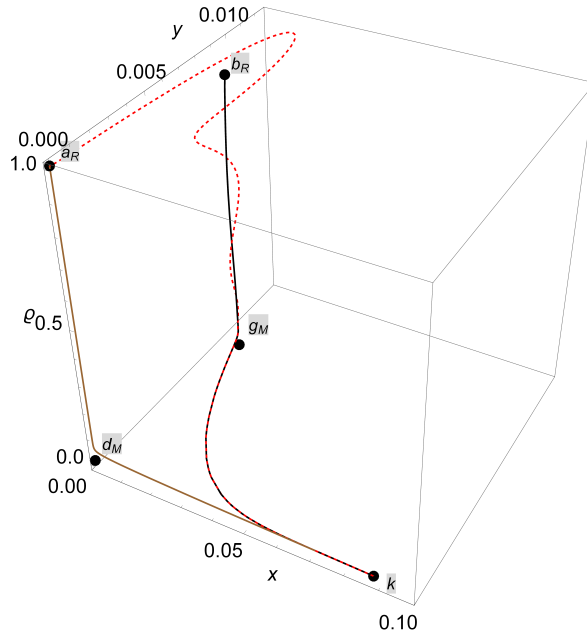


**Figure 3.** We plot the physical evolution curves in the phase space for the values of parameter  $s = -1.20$ ,  $\sigma = 0.3$  and  $\lambda = 150$ , and for the three different set of initial conditions  $x_i = 1 \times 10^{-9}$ ,  $y_i = 4 \times 10^{-7}$ ,  $z_i = 9.1 \times 10^{-30}$ ,  $\varrho_i = 0.999877$  (red dashed),  $x_i = 1 \times 10^{-33}$ ,  $y_i = 1 \times 10^{-41}$ ,  $z_i = 1.05 \times 10^{-29}$ ,  $\varrho_i = 0.999877$  (brown), and  $x_i = 0.0108$ ,  $y_i = 0.00765$ ,  $z_i = 9.3 \times 10^{-30}$ ,  $\varrho_i = 0.999788$  (black)

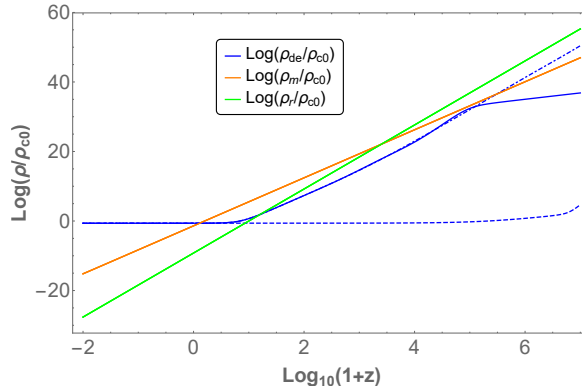


**Figure 4.** We depict the evolution of the energy density of dark energy  $\rho_{de}$  (blue), dark matter (including baryons)  $\rho_m$  (orange) and radiation  $\rho_r$  (green) as functions of the redshift  $z$ , for  $s = -0.8$ ,  $\sigma = 17$  and  $\lambda = 0.01$ . The dashed line corresponds to the initial conditions  $x_i = 1 \times 10^{-11}$ ,  $y_i = 7.3 \times 10^{-13}$ ,  $z_i = 1 \times 10^{-8}$ ,  $\varrho_i = 0.999875$ , solid blue line to  $x_i = 1 \times 10^{-8}$ ,  $y_i = 7.3 \times 10^{-13}$ ,  $z_i = 1 \times 10^{-23}$ ,  $\varrho_i = 0.999875$ , and dot-dashed blue line to  $x_i = 0.0768467$ ,  $y_i = 7.3 \times 10^{-13}$ ,  $z_i = 0.002$ ,  $\varrho_i = 0.995916$ . It is observed the two new scaling regimes during the radiation and dark matter era. To obtain this plot we have found the current values for the fractional energy densities of dark energy  $\Omega_{de}^{(0)} = 0.68$  and dark matter  $\Omega_m^{(0)} = 0.32$ , at redshift  $z = 0$ , according to Planck results [3]. Also, during the scaling radiation epoch we have imposed the BBN constraint  $\Omega_{de}^{(r)} < 0.045$  [56], and the constraint for the field energy density during the scaling matter epoch  $\Omega_{de}^{(m)} < 0.02$  (95% C.L.), at redshift  $z \approx 50$ , from CMB measurements [57].

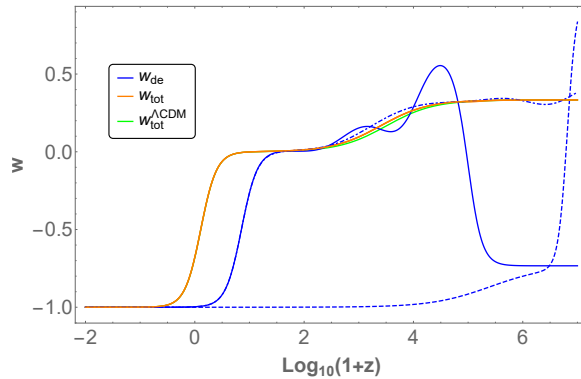


**Figure 5.** It is shown the behaviour of the total equation of state  $w_{tot}$  (orange line), the equation of state of dark energy  $w_{de}$  (blue line), and the total equation of state of  $\Lambda$ CDM model (green line) as functions of the redshift  $z$  for the values of parameters for  $s = -0.8$ ,  $\sigma = 17$  and  $\lambda = 0.01$ . Also, for solid, dashed, and dot-dashed blue lines we have the same initial conditions of FIG. 4. It is observed the value  $w_{de} \approx -0.997$  at the current time  $z = 0$ , which is consistent with the observational constraint  $w_{de}^{(0)} = -1.028 \pm 0.032$ , from Planck [3].

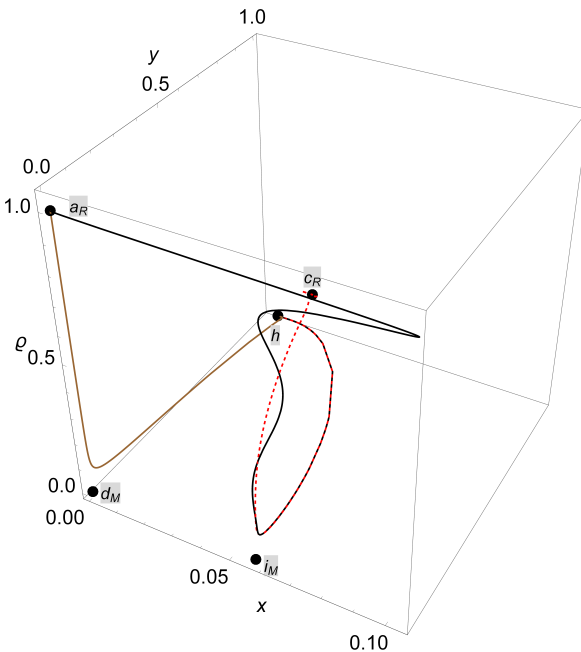


**Figure 6.** We plot the physical evolution curves in the phase space for the values of parameter  $s = -0.8$ ,  $\sigma = 17$  and  $\lambda = 0.01$ , and for the three different set of initial conditions  $x_i = 1 \times 10^{-11}$ ,  $y_i = 7.3 \times 10^{-13}$ ,  $z_i = 1 \times 10^{-8}$ ,  $\rho_i = 0.999875$  (brown),  $x_i = 1 \times 10^{-8}$ ,  $y_i = 7.3 \times 10^{-13}$ ,  $z_i = 1 \times 10^{-23}$ ,  $\rho_i = 0.999875$  (black), and  $x_i = 0.0768467$ ,  $y_i = 7.3 \times 10^{-13}$ ,  $z_i = 0.002$ ,  $\rho_i = 0.995916$  (red dashed).

## 8 Concluding Remarks

In the present work we have investigated the cosmological dynamics of dark energy in the context of scalar-torsion  $f(T, \phi)$  gravity, where  $f(T, \phi)$  is a function of the torsion scalar  $T$ , associated with the Weitzenböck connection in the context of modified teleparallel gravity, and the scalar field  $\phi$ . Particularly, we have studied the class of theories with Lagrangian density  $f(T, \phi) = -T/2\kappa^2 - F(\phi)G(T) - V(\phi)$ , with  $F(\phi) \sim e^{-\sigma\kappa\phi}$ ,  $V(\phi) \sim e^{-\lambda\kappa\phi}$  and  $G(T) \sim T^{1+s}$ , plus the canonical kinetic term for the scalar field. The exponential scalar potential is the usual one studied in the context of dark energy which admits scaling solutions, while the exponential coupling function of the scalar field is the simplest natural choice to be assumed with this potential [41]. Furthermore, the function  $G(T)$  generalizes to the non-linear case the typical choice of a linear function in  $T$  for the nonminimal coupling to gravity [44, 45]. It has been shown in Ref. [38], that in order to generate primordial fluctuations during inflation from  $f(T, \phi)$  gravity, non-linear terms in torsion scalar need to be considered to construct the coupling function, when the nonminimal coupling to gravity is switch on. So, for the FLRW background, and in the presence of radiation and cold dark matter, we have defined the effective energy and pressure densities of dark energy. Thus, we have obtained the autonomous system associated with the set of cosmological equations and then we have performed the dynamical analysis in the phase space for the cosmological model at hand, by getting the critical points, their cosmological properties and stability conditions.

Some interesting features have been found that make the model appealing as a viable dark energy candidate. For  $s \neq 0$ , we have found the existence of new attractors solutions describing the dark energy dominated era and new scaling solutions representing the scaling radiation and scaling dark matter eras. So, since the latter are saddle points, we have scaling regimes during the radiation and cold dark matter epochs followed by the dark energy attractor with accelerated expansion. In FIGS. 1 and 4, as well as in FIGS. 3, and 6, we have numerically confirmed that the dynamics of the model can allow the two scaling regimes previous to the dark energy dominated epoch, satisfying the cosmological constraints for the early-time dark energy density from BBN [56] and CMB bounds [3]. Therefore, the final attractor can be either a de Sitter solution ( $w_{de} = -1$ ), or a dark energy dominated solution with  $\Omega_{de} = 1$ , and equation of state with quintessence-like, phantom-like behaviour or experiencing the phantom-divide crossing, as it has been illustrated in FIGS 2 and 5. We also have found some ranges for the parameters of the scaling solutions, where, these solutions can also be attractors, but in this case, they cannot explain the current accelerated expansion. On other other hand, the phantom-divide crossing during the cosmological evolution indicates a distinctive feature of the model as compared with minimally coupled scalar field in GR, and that has been inherited from the case with  $s = 0$  [44].

Finally, we would like to highlight that for the present model to be a good candidate for description of our Universe, it must be verified that it is free from any theoretical pathologies, such as ghost, gradient and tachyonic instabilities, through a rigorous stability analysis in the presence of matter fields [58], as well as, it is necessary to perform a detailed comparison with cosmological observations, e.g. SNIa, BAO,  $H(z)$ , CMB, LSS, etc [59], and Solar System data, after extracting spherically symmetric solutions [30]. These necessary studies lie beyond the scope of the present work and thus are left for separated projects.

## Acknowledgments

G. Otalora acknowledges DI-VRIEA for financial support through Proyecto Postdoctorado 2020 VRIEA-PUCV. M. Gonzalez-Espinoza acknowledges support from PUCV.

## References

- [1] A.G. Riess, et al., *Astron. J.* **116**, 1009 (1998)
- [2] S. Perlmutter, et al., *Astrophys. J.* **517**, 565 (1999)
- [3] N. Aghanim, et al., *Astron. Astrophys.* **641**, A6 (2020)
- [4] J. Solà, A. Gómez-Valent, J. de Cruz Pérez, *Phys. Lett.* **B774**, 317 (2017)
- [5] L. Kazantzidis, L. Perivolaropoulos, *Phys. Rev.* **D97**(10), 103503 (2018)
- [6] I. Albarran, M. Bouhmadi-López, J. Morais, *Phys. Dark Univ.* **16**, 94 (2017)
- [7] E. Di Valentino, et al., arXiv:2008.11283 (2020)
- [8] E. Di Valentino, et al., arXiv:2008.11284 (2020)
- [9] E. Di Valentino, et al., arXiv:2008.11285 (2020)
- [10] E. Di Valentino, et al., arXiv:2008.11286 (2020)
- [11] V. Faraoni, *Cosmology in scalar-tensor gravity*, vol. 139 (Springer Science & Business Media, 2004)
- [12] T. Kobayashi, arXiv:1901.07183 [gr-qc] (2019)
- [13] T. Baker, E. Bellini, P.G. Ferreira, M. Lagos, J. Noller, I. Sawicki, *Phys. Rev. Lett.* **119**(25), 251301 (2017)
- [14] J. Sakstein, B. Jain, *Phys. Rev. Lett.* **119**(25), 251303 (2017)
- [15] E. Di Valentino, A. Melchiorri, O. Mena, S. Vagnozzi, *Phys. Dark Univ.* **30**, 100666 (2020)
- [16] E. Di Valentino, A. Melchiorri, O. Mena, S. Vagnozzi, *Phys. Rev. D* **101**(6), 063502 (2020)
- [17] L. Amendola, M. Quartin, S. Tsujikawa, I. Waga, *Phys. Rev. D* **74**, 023525 (2006)
- [18] I.S. Albuquerque, N. Frusciante, N.J. Nunes, S. Tsujikawa, *Phys. Rev. D* **98**(6), 064038 (2018)
- [19] A. Gomes, L. Amendola, *JCAP* **03**, 041 (2014)
- [20] T. Chiba, A. De Felice, S. Tsujikawa, *Phys. Rev. D* **90**(2), 023516 (2014)
- [21] A. De Felice, S. Tsujikawa, *Living Rev. Rel.* **13**, 3 (2010)
- [22] T.P. Sotiriou, V. Faraoni, *Rev. Mod. Phys.* **82**, 451 (2010)
- [23] S. Nojiri, S.D. Odintsov, *Phys. Rept.* **505**, 59 (2011)
- [24] L. Amendola, S. Tsujikawa, *Dark energy: theory and observations* (Cambridge University Press, 2010)
- [25] S. Capozziello, V. Faraoni, *Beyond Einstein gravity: A Survey of gravitational theories for cosmology and astrophysics*, vol. 170 (Springer Science & Business Media, 2010)
- [26] J.G. Pereira, in *Handbook of Spacetime*, ed. by A. Ashtekar, V. Petkov (Springer, 2014), pp. 197–212
- [27] V.C. de Andrade, L.C.T. Guillen, J.G. Pereira, *Phys. Rev. Lett.* **84**, 4533 (2000)
- [28] H.I. Arcos, J.G. Pereira, *Int. J. Mod. Phys. D* **13**, 2193 (2004)

- [29] J.G. Pereira, Y.N. Obukhov, *Universe* **5**(6), 139 (2019)
- [30] L. Iorio, E.N. Saridakis, *Mon. Not. Roy. Astron. Soc.* **427**, 1555 (2012)
- [31] L. Iorio, N. Radicella, M.L. Ruggiero, *JCAP* **08**, 021 (2015)
- [32] G. Farrugia, J. Levi Said, M.L. Ruggiero, *Phys. Rev. D* **93**(10), 104034 (2016)
- [33] S. Peirone, G. Benevento, N. Frusciante, S. Tsujikawa, *Phys. Rev.* **D100**(6), 063509 (2019)
- [34] M. Gonzalez-Espinoza, G. Otalora, J. Saavedra, N. Videla, *Eur. Phys. J. C* **78**(10), 799 (2018)
- [35] T. Harko, F.S.N. Lobo, G. Otalora, E.N. Saridakis, *Phys. Rev. D* **89**, 124036 (2014)
- [36] T. Harko, F.S.N. Lobo, G. Otalora, E.N. Saridakis, *JCAP* **12**, 021 (2014)
- [37] N.D. Birrell, N.D. Birrell, P. Davies, P. Davies, *Quantum fields in curved space* (Cambridge university press, 1984)
- [38] M. Gonzalez-Espinoza, G. Otalora, *Phys. Lett. B* **809**, 135696 (2020)
- [39] Y.P. Wu, C.Q. Geng, *Phys. Rev. D* **86**, 104058 (2012)
- [40] J.P. Uzan, *Phys. Rev. D* **59**, 123510 (1999)
- [41] L. Amendola, *Phys. Rev. D* **60**, 043501 (1999)
- [42] R. Aldrovandi, J.G. Pereira, *Teleparallel gravity: an introduction*, vol. 173 (Springer Science & Business Media, 2012)
- [43] S. Weinberg, *Gravitation and Cosmology: Principles and Applications of the General Theory of Relativity* (John Wiley and Sons, New York, 1972)
- [44] C.Q. Geng, C.C. Lee, E.N. Saridakis, Y.P. Wu, *Phys. Lett. B* **704**, 384 (2011)
- [45] G. Otalora, *JCAP* **1307**, 044 (2013)
- [46] G. Otalora, *Phys. Rev. D* **88**, 063505 (2013)
- [47] G. Otalora, *Int. J. Mod. Phys. D* **25**(02), 1650025 (2015)
- [48] M.A. Skugoreva, E.N. Saridakis, A.V. Toporensky, *Phys. Rev. D* **91**, 044023 (2015)
- [49] G.R. Bengochea, R. Ferraro, *Phys. Rev.* **D79**, 124019 (2009)
- [50] E.V. Linder, *Phys. Rev.* **D81**, 127301 (2010)
- [51] B. Li, T.P. Sotiriou, J.D. Barrow, *Phys. Rev. D* **83**, 104017 (2011)
- [52] Y.F. Cai, S. Capozziello, M. De Laurentis, E.N. Saridakis, *Rept. Prog. Phys.* **79**(10), 106901 (2016)
- [53] E.J. Copeland, M. Sami, S. Tsujikawa, *Int. J. Mod. Phys. D* **15**, 1753 (2006)
- [54] S. Bahamonde, C.G. Böhmmer, S. Carloni, E.J. Copeland, W. Fang, N. Tamanini, *Phys. Rept.* **775-777**, 1 (2018)
- [55] P.G. Ferreira, M. Joyce, *Phys. Rev. D* **58**, 023503 (1998)
- [56] R. Bean, S.H. Hansen, A. Melchiorri, *Phys. Rev. D* **64**, 103508 (2001)
- [57] P. Ade, et al., *Astron. Astrophys.* **594**, A14 (2016)
- [58] A. De Felice, N. Frusciante, G. Papadomanolakis, *JCAP* **03**, 027 (2017)
- [59] Z. Davari, V. Marra, M. Malekjani, *Mon. Not. Roy. Astron. Soc.* **491**(2), 1920 (2020)